Modeling instabilities in lean premixed turbulent combustors using detailed chemical kinetics

Bjørn Lilleberg, Ivar S. Ertesvåg* and Kjell Erik Rian

Department of Energy and Process Engineering,
Norwegian University of Science and Technology
N-7491 Trondheim, Norway

∗ E-mail: Ivar.S.Ertesvag@ntnu.no
Fax.No.: +47 73 59 35 80

ABSTRACT

Development of non-conventional combustion technology with ultra-low emissions and safe operation of combustion systems require a thorough understanding of the mechanisms of combustion instabilities. The objective of the present work is to investigate the role of unmixedness and chemical kinetics in driving combustion instabilities. The reaction-rate responses of different species to inlet flow variations have been studied using a perfectly stirred reactor model. Transient simulations of combustion of methane and propane with air, using both global single-step and detailed chemical kinetic mechanisms, have been conducted with imposed oscillations on inflow mass flow rate, temperature and mixture equivalence ratio. The detailed mechanisms predicted fuel reaction-rate oscillations with amplitudes proportional to the imposed oscillations. However, increased amplitudes of the reaction rates of CO_2 and OH where observed when the combustion became leaner, while the reaction-rate amplitudes of CO and H_2 decreased. The single-step mechanisms predicted to some degree a similar reaction-rate behavior as the detailed mechanisms. However, near stoichiometric conditions the fuel reaction rate of propane showed little influence by the imposed oscillations. When the mean equivalence ratio was lowered below a certain value, the fuel reaction-rate oscillations grew stronger and became larger than seen with the detailed mechanism. This shows that simple mechanisms can by themselves introduce instabilities not seen with detailed mechanisms.

1 INTRODUCTION

More stringent emission regulations drive the new generation of gas turbines to leaner premixed operation in order to lower the combustion temperature and thereby the NO_x formation. However, lean premixed combustors are susceptible to thermoacoustic oscillations and other instabilities. These combustion instabilities are characterized by oscillations of one or more natural acoustic modes of the combustor. The driving mechanism behind these instabilities in gas turbine combustors is a result of complex feedback-type interactions between a periodic flow field, chemical kinetics, heat release and pressure fluctuations. However, the details of the mechanisms leading to amplification, self-sustenance and damping of the oscillations are not very well understood. These combustion instabilities produce system vibrations, enhanced heat transfer and thermal stresses to the combustor walls and flame blowoff or flashback (Poinsot and Veynante, 2005; Zinn and Lieuwen, 2005).

In the present study an in-house code using an unsteady perfectly stirred reactor (PSR) model has been developed to investigate the role of unmixedness and chemical kinetics in driving combustion instabilities of lean premixed combustion. This work follows up the work reported by Lieuwen et al. (1998), who studied the transient development of reaction-rate oscillations produced by periodic flow rate, temperature and equivalence ratio variations in the combustor inlet flow at different mean equivalence ratios. In an experimental study on the influence of reactant unmixedness on combustion stability, Shih et al. (1996) found that instabilities occured near stoichiometric conditions, whereas for lean mixtures the combustor was stable. On the other hand, experiments by Cohen and Anderson (1996) have shown that the amplitude of the pressure oscillations increased as the combustor was operated at leaner mixtures. Using a global single-step kinetic mechanism for propane, Lieuwen et al. (1998) concluded that periodic variations in equivalence ratio play a key role in driving combustion instabilities for lean premixed conditions. Prior to the present study, some preliminary investigations on combustion instabilities were performed by Myhrvold and Gruber (2006).

In the present work the responses of the model to variations in flow rate, temperature and equivalence ratio have been tested. Moreover, a global chemical kinetic mechanism for propane and a detailed kinetic mechanism for propane are compared, and the same is done for methane.

2 REACTOR MODELING

2.1 Unsteady perfectly stirred reactor

The perfectly stirred reactor regime for turbulent premixed combustion is characterized by fast turbulent mixing where the characteristic times of the turbulent motions are shorter than the chemical reaction time (Williams, 1985; Borghi, 1988). In an unsteady perfectly stirred reactor (PSR) model, perfect mixing is achieved instantaneously inside the combustor, and the properties inside the combustor are uniform. That is, spatial gradients are disregarded (Turns, 2000). Details of convection and mixing processes are also neglected. The advantage of using a PSR-model for premixed turbulent combustion is that effects of chemical kinetics are isolated and in detail. The governing equations for

the PSR model can be expressed as

$$\frac{dY_i}{dt} = \frac{1}{\tau}(Y_{i,\text{in}} - Y_i) + \frac{R_i}{\rho} \qquad i = 1, \ldots, N_S \tag{1}$$

$$\frac{dh}{dt} = \frac{1}{\tau}(h_{\text{in}} - h) + Q \tag{2}$$

$$\frac{dp}{dt} = 0 \tag{3}$$

where the reciprocal of the time scale is defined as

$$\frac{1}{\tau} = \frac{\dot{m}_{\text{in}}}{m_R} = \frac{\dot{m}_{\text{in}}}{(\rho \cdot V_R)} \tag{4}$$

and the mass density ρ and the species volumetric reaction rate R_i are function of temperature, pressure and composition. Here, t, Y_i, h, p and Q refer to time, species mass fraction, specific enthalpy, pressure and heat transfer rate, respectively. The index i refers to chemical species, N_S is the number of species and the subscript "in" refers to conditions at the reactor inlet. τ is the reactor residence time and $\dot{m}_{\text{in}}$, m_R and V_R are the mass flow rate into the reactor, the mass inside the reactor and the reactor volume, respectively. The perfectly stirred reactor is sketched in Fig. 1. Equations (1)-(3) of the PSR model are the same as those used in the Eddy Dissipation Concept for turbulent combustion (Gran and Magnussen, 1996) for detailed chemistry calculations. Lieuwen et al. (1998) also used an unsteady PSR model similar to Eqs. (1)-(3) expressing the energy balance (Eq. (2)), in terms of the temperature, T. In the present work, an equation for the mixture enthalpy is used, and the mixture temperature is found from the mixture enthalpy and composition by Newton iteration. In order to obtain results that are independent of geometry-specific system dynamics, no feedback was included in the PSR model. This open-loop response of the combustor to inlet flow variations makes the results more general.

Regarding the reactor residence time, τ, there are different combinations of what could be held constant, see Table 1. Here, we have chosen to restrict the investigation to Mode I, as in the work of Lieuwen et al. (1998).

2.2   Chemical models

The chemistry of methane-air and propane-air combustion have been modeled by global single-step and detailed finite-rate chemical mechanisms. The reaction rate for a single-step global reaction can be written (Turns, 2000) as

$$R_{\text{fuel}} = -A \cdot \rho^{m+n} \cdot Y_{\text{fuel}}^m \cdot Y_{O_2}^n \cdot \exp(-T_a/T) \tag{5}$$

where A, m, n and T_a are parameters given by curve fitting to experimental data. Expressions like Eq. (5) are valid within certain ranges of equivalence ratio and temperature.

A detailed mechanism for simple hydrocarbons comprises a large number of elementary reactions and chemical species, where each reaction is modeled similar to Eq. (5).

3 PRESENT CALCULATIONS

3.1 General assumptions and chemical mechanisms

The integration of Eqs. (1)-(3) was done with the Runge-Kutta scheme RADAU5 (Hairer and Wanner, 1996, 2002). The constant pressure in the PSR was set to 1.0 atm, and the reactor was regarded as adiabatic.

For the detailed chemistry calculations, GRI-Mech 3.0 (Smith et al., 1999) was used for the methane-air (21% O_2 and 79% N_2) combustion. This mechanism, comprising 325 elementary reactions and 53 species, is designed to model a variety of natural gas compositions in industrial combustors. For the propane-air (21% O_2 and 79% N_2) combustion, the San-Diego mechanism (2005) with 235 elementary reactions and 46 species was used. CHEMKIN subroutines (Kee et al., 1996) were applied for the calculation of the chemical reaction rates from the detailed mechanisms. Thermophysical data were evaluated using CHEMKIN subroutines and data distributed with the respective mechanisms. For the simulations with the global single-step mechanisms, thermophysical data distributed with the GRI-Mech 3.0 mechanism were used.

The constants applied in the global single-step chemical mechanisms, are given in Table 2. West-brook (1981) computed the flammability limits for the single-step propane mechanism to $\phi_{\text{lean}} = 0.5$ and $\phi_{\text{rich}} = 3.2$.

3.2 Validation of the reactor model

For initial testing of the numerical simulation code with the unsteady PSR model, the inlet flow properties were specified. The inlet flow temperature was gradually increased until ignition of the mixture, letting the inlet flow temperature drop back to 300 K, and then integrating in time until a steady-state solution was reached. Details of the ignition procedure are explained in the next section. The equivalence ratio of the mixture was varied between 1.0 and 0.7. This was conducted for the detailed and single-step mechanisms for both propane and methane. For methane, the mechanism with unity exponents (Table 2) was used.

The steady-state reactor temperature, T, and the mixture composition, Y_i, were compared to results from an STANJAN-based Chemical Equilibrium Calculator (2007). The equilibrium calculations of the various mixtures of air and fuel were done with constant enthalpy and pressure (1.0 atm), as in the PSR numerical code. The additional species in the calculator were CO_2 and H_2O for the global single-step mechanisms. For comparison with the detailed mechanisms the species from the PSR calculations were sorted from largest to smallest mole fraction and included in the equilibrium calculations until the maximum number of allowed species in the equilibrium calculator was reached, that is, 30 species in addition to the input species (fuel, O_2 and N_2).

3.3 Ignition and extinction

The transient performance of the numerical code was tested by simulating ignition and extinction of the reactor. A time-dependent inlet flow temperature was defined (Lieuwen et al., 1998) as

$$
T_{\text{in}} = \begin{cases} 300 + a \cdot (0.025t - t^2)\,\text{K} & \text{for} \quad 0 < \quad t < 0.011\,\text{s} \\ 300\,\text{K} & \text{for} \qquad\quad t \geq 0.011\,\text{s} \end{cases} \tag{6}
$$

where the different values used for the constant a are given in Table 3. Furthermore, a time-dependent inlet equivalence ratio was stated (Lieuwen et al., 1998) as

$$
\phi_{\text{in}} = \begin{cases} 1.0 & \text{for} \quad 0 < \quad t < 0.025\,\text{s} \\ 1.4 - 16 \cdot t & \text{for} \qquad\quad t \geq 0.025\,\text{s} \end{cases} \tag{7}
$$

For these simulations the ratio $\dot{m}_{\text{in}}/V_{\text{R}}$ were kept constant at $500\,\text{kg/(m}^3\text{s)}$, cf. Eq. (4).

3.4 Periodic variations of the PSR inlet conditions

Following the investigations by Lieuwen et al. (1998), simulations with periodic variations of the PSR inlet were performed. In each case, either the equivalence ratio, the temperature or the mass flow rate was periodically varied as

$$
\begin{align}
\phi_{\text{in}} &= \phi_{\text{mean}} \cdot (1 + \alpha_\phi \cdot \cos(2\pi \cdot f \cdot t)) \tag{8} \\
T_{\text{in}} &= T_{\text{mean}} \cdot (1 + \alpha_{\text{T}} \cdot \cos(2\pi \cdot f \cdot t)) \tag{9} \\
\dot{m}_{\text{in}}/V_{\text{R}} &= (\dot{m}_{\text{in}}/V_{\text{R}})_{\text{mean}} \cdot (1 + \alpha_{\text{m}} \cdot \cos(2\pi \cdot f \cdot t)) \tag{10}
\end{align}
$$

For all these simulations, a stoichiometric mixture was first ignited and then the mean equivalence ratio was linearly reduced from $\phi_{\text{mean}} = 1.0$ (at $t = 0.05\,\text{s}$) to $\phi_{\text{mean}} = 0.73$ (at $t = 0.4\,\text{s}$) to allow the PSR to respond in a quasi-steady manner and the frequency $f = 100\,\text{Hz}$ (Lieuwen et al., 1998).

Simulations were conducted with inlet mean temperatures of 300, 600 and 900 K and inlet mean flow rates of 300, 500 and $1000\,\text{kg/(m}^3\text{s)}$. The amplitudes of the oscillating inlet equivalence ratio, α_ϕ, were 1%, 2.5%, 5% and 7.5%, the amplitudes of the oscillating inlet temperature, α_{T}, were 5%, 10%, 15% and 20%, and the amplitudes of the inlet flow rate, α_{m}, were 3%, 5%, 7% and 10%. This made a total of 108 cases for each of the chemical mechanisms. The global single-step methane mechanism with non-unity exponents (Methane (2) in Table 2) was only tested for some of these amplitudes. The other four mechanisms were tested for all 108 cases.

In addition the frequency dependence of the normalized reaction-rate response (i.e., normalized by the response at $0\,\text{Hz}$) to equivalence ratio oscillations was studied.

4 RESULTS

4.1 Validation of the reactor model

In the initial reactor tests of the propane-air and methane-air mixtures with respective mechanisms, the equilibrium solution obtained with the unsteady PSR numerical code (setting $\tau = 1.0\,\text{s}$) showed very

good agreement with the results from the STANJAN-based Chemical Equilibrium Calculator (2007). The maximum temperature difference between the equilibrium calculations and the PSR calculations was $5.6\,\mathrm{K}$. However, the global single-step propane mechanism failed to work for $\phi < 1.0$ with $\tau = 1.0\,\mathrm{s}$. For $\phi = 0.90$, the residence time τ had to be set to approximately $7 \cdot 10^{-4}\,\mathrm{s}$ in order to avoid integrator failure.

4.2 Ignition and extinction

Figure 2 shows the results of the ignition and extinction simulations. It is observed that the PSR temperature, T, follows the inlet flow temperature until ignition, reaches a steady-state and then is reduced according to the subsequent reduction in the inlet equivalence ratio, ϕ_{in}. When the mixture reaches the lean limit, the reactor extinguishes and T drops towards T_{in}. Figure 2 (solid line) shows the PSR temperature predicted by the San-Diego and GRI-Mech 3.0 mechanisms. The development in time when using the detailed mechanisms is quite similar and extinction occurs at approximately $0.055\,\mathrm{s}$.

When using the global single-step kinetic mechanisms for propane and methane, the temperature predicted was higher than the temperature predicted using the detailed mechanisms, see Fig. 2. The two global single-step kinetic mechanisms for methane gave nearly the same time-development and only the result for the mechanism with unity mass-fraction exponents is shown.

The present results from using the global single-step propane mechanism were in qualitatively good agreement with the corresponding simulations by Lieuwen et al. (1998). However, they reported a predicted steady-state temperature of approximately $1950\,\mathrm{K}$ for $\phi_{\mathrm{in}} = 1.0$, whereas the corresponding temperature found here was approximately $2170\,\mathrm{K}$. The reason for the lower temperature by Lieuwen et al. (1998) is not known although incomplete combustion can be a possible explanation. The difference in predicted temperatures also affects the extinction times, as a higher temperature delays the extinction.

Furthermore, a small increase in temperature was observed for the single-step propane mechanism between $0.025\,\mathrm{s}$ and $0.035\,\mathrm{s}$ in Fig. 2a. This was a result of delayed combustion of unburned propane in the reactor. After $0.035\,\mathrm{s}$, almost all the propane was consumed and the burned mixture was cooled by the excess air. The results of the San-Diego mechanism did not show this increase in temperature. For the simulation with the single-step kinetic mechanisms for methane, there was no increase in temperature as the mixture was made leaner. Almost all the methane was consumed at the steady-state stage. Similar to the simulations with propane, the simulation of methane combustion with GRI-Mech 3.0 gave extinction earlier than with the single-step mechanism, but the difference in the equivalence ratio at extinction was larger than for the propane cases.

The calculations with the Chemical Equilibrium Calculator (2007) for propane-air combustion gave a maximum adiabatic flame temperature at $\phi = 1.05$ (rich mixture). This is shown by Turns (2000) (p. 46), as well. Calculations with the San-Diego mechanism also showed a peak in temperature at $\phi_{\mathrm{in}} = 1.05$ when ϕ_{in} was increased from 1.0 to 1.1 (with $\tau = 1.0\,\mathrm{s}$). On the other hand, the global single-step propane mechanism showed a decrease in T for all ϕ_{in} larger than unity.

5

4.3 Variations of the inflow equivalence ratio, ϕ_{in}

The results of the simulations presented here are based on $T_{\mathrm{in}} = 300\,\mathrm{K}$, $\dot{m}_{\mathrm{in}}/V_{\mathrm{R}} = 500\,\mathrm{kg/(m^3 s)}$ and a 2.5% or a 5.0% oscillation of the inflow equivalence ratio. Figure 3 shows how the PSR responded to a 2.5% variation in the equivalence ratio. The reaction-rate response for propane combustion predicted by the San-Diego mechanism is shown in Fig. 3a. The result for methane combustion with the GRI-Mech 3.0 mechanism is not shown here since the reaction-rate response was very similar to that seen in Fig. 3b. As Fig. 3 shows, the oscillations of the propane and methane consumption rates had an almost constant amplitude for the whole time-range. Figures 4a-c show graphs of CO, CO_2 and OH reaction-rate oscillations due to a 5% variation about ϕ_{mean} (also shown in the graphs) using the San-Diego mechanism. The results for the two detailed mechanisms showed the same trends for each species. For both mechanisms the oscillations in the reaction rates of CO_2 and OH increased with decreasing ϕ_{mean}, while the oscillations in the reaction rate of CO and H_2 decreased. CO and H_2 had the same evolution in time. For $t < 0.1\,\mathrm{s}$, the oscillations in the reaction rate of OH were somewhat damped. As for H_2O, the amplitude of the reaction-rate oscillations was nearly constant (not shown here, approximately 80% of the mean reaction rate of CO_2). Compared to the oscillating reaction rate of the fuel, the reaction-rate amplitude of the other species varied much more from rich to lean mixtures.

The results for the global propane mechanism were qualitatively in excellent accordance with those reported by Lieuwen et al. (1998) and showed that the reaction-rate oscillations increased significantly as the equivalence ratio decreased. As can be seen in Fig. 3a, the amplitude of the oscillating reaction rate of propane went to zero at $t \approx 0.15\,\mathrm{s}$ when using the global single-step mechanism. From the mass fractions of C_3H_8 and O_2, temperature and density, it was observed that there was excess of propane leaving the reactor between $t = 0.05\,\mathrm{s}$ and $t \approx 0.15\,\mathrm{s}$. This incomplete combustion was due to the short residence time. The reaction-rate oscillations were in phase with the C_3H_8 mass fraction and the density oscillations, and out of phase with the O_2 mass fraction and temperature oscillations. The temperature reached its maximum at $t \approx 0.15\,\mathrm{s}$ when most of the fuel was consumed. At $t \approx 0.15\,\mathrm{s}$, the C_3H_8 and O_2 mass-fraction oscillations started competing (being in opposite phases), and hence the resulting reaction-rate amplitude went to zero. After $t \approx 0.15\,\mathrm{s}$, the incoming mixture was so fuel-lean that almost all C_3H_8 was consumed, and the resulting reaction-rate oscillations were in phase with the O_2 mass fraction and the density ρ. In this time-range ($t > 0.15\,\mathrm{s}$), the temperature decreased because the mixture was diluted with excess air and less fuel flowed into the reactor. Investigating Eq. (5) (cf. Table 2) for the global propane mechanism, the variation in $Y_{C_3H_8}$ and temperature appeared to neutralize each other giving a nearly constant reaction rate for the time interval $0.05\,\mathrm{s}$ to $0.15\,\mathrm{s}$. Y_{O_2} and ρ were nearly constant for the same time interval. After this, almost all the fuel was consumed, the mass fraction of O_2 increased, the temperature decreased, density increased and the reaction rate decreased more or less linearly with time. From $t \approx 0.25\,\mathrm{s}$, the amplitude of the reaction-rate oscillation was constant.

Because of the nature of the global single-step kinetic mechanisms for methane (unity or near-unity exponents for Y_{O_2} and Y_{CH_4}) and some excess methane in the reactor for $t < 0.1\,\mathrm{s}$, the reaction rate was a little damped due to lack of O_2, see Fig. 3b. For the remaining time-range, both the global and the detailed mechanism gave a methane reaction rate for which the oscillations had an almost constant amplitude. When running the same test with the global methane mechanism with non-unity exponents, the equivalence ratio had to be kept below unity due to numerical limitations.

When Figs. 3 and 4 are compared, it is observed that the detailed propane mechanism did not pre-

dict the large increase in reaction-rate oscillations seen with the global propane mechanism. The increase in the reaction-rate oscillations for CO_2, see Figs. 4b and d, was not as fast as predicted by the global propane mechanism. The H_2O reaction-rate amplitude predicted by the detailed mechanism was constant. The global propane mechanism is clearly not reproducing all the features of the detailed mechanism. Adjusting the exponents to the mass fractions in the expression for the global propane mechanism towards unity, the reaction-rate response became more and more like the response predicted by the other mechanisms. Similarly, when the mass-fraction exponent for oxygen in the non-unity global methane mechanism was adjusted from 0.8 towards 2.0, the reaction-rate response became more and more like the response of the global propane mechanism.

Simulations with other imposed oscillation amplitudes (cf. Sec. 3.4) showed that the magnitude of the reaction-rate amplitude varied linearly with the amplitude of the imposed oscillation. However, using the global propane mechanism with $\dot{m}_{in}/V_R = 300\,\mathrm{kg/(m^3s)}$ and $T_{in} = 600\,\mathrm{K}$, $\dot{m}_{in}/V_R = 300\,\mathrm{kg/(m^3s)}$ and $T_{in} = 900\,\mathrm{K}$, and $\dot{m}_{in}/V_R = 500\,\mathrm{kg/(m^3s)}$ and $T_{in} = 900\,\mathrm{K}$, led to numerical problems and integrator failure.

4.4 Frequency dependence of the reaction-rate response

Figure 5 shows the frequency dependence of the normalized reaction-rate response (i.e., normalized by the response at $0\,\mathrm{Hz}$) for C_3H_8 and H_2O to equivalence ratio oscillations using the San-Diego mechanism (2005). As in the simulations reported by Lieuwen et al. (1998), the simulations presented here are based on $T_{in} = 300\,\mathrm{K}$, $\dot{m}_{in}/V_R = 400\,\mathrm{kg/(m^3s)}$ and ϕ_{mean} equal to 0.95 or 0.7 with 5.0% oscillation of the inflow equivalence ratio. When the frequencies are larger than the inverse of the reactors residence time the normalized reaction-rate response asymptotically approach a constant value. Simulations were also done using the single-step propane mechanism and the results were similar to what Lieuwen et al. (1998) reported.

4.5 Variations in inlet flow rate, $\dot{m}_{in}/V_R$

Next, the reaction-rate responses to periodic inlet flow-rate variations were tested. Here, the results for $(\dot{m}_{in}/V_R)_{mean} = 500\,\mathrm{kg/(m^3s)}$ and $T_{in} = 300\,\mathrm{K}$ with a 5.0% variation in $\dot{m}_{in}/V_R$ will be presented. The reaction-rate oscillations for C_3H_8, CO_2, OH obtained from the detailed San-Diego mechanism are shown in Figs. 6a-c. The different species oscillating reaction rates have the same transient trends as shown in Figs. 3a and 4b-c, and described in the previous section, but the amplitudes are almost constant. Only a minor decrease was observed as the mean equivalence ratio decreased. The same was observed for amplitudes of the oscillations of methane and propane, with respective detailed mechanisms. Near stoichiometric conditions, the propane, see Fig. 6d, and methane reaction-rate amplitudes were 1.3 and 1.4 times larger than in Fig. 3.

Results for the propane reaction rate with the global single-step mechanism shown in Fig. 6d were in good agreement with the simulations reported by Lieuwen et al. (1998). The transient development of the C_3H_8 reaction rate showed a flat profile in the beginning. The reason for this was the same as described in Sec. 4.3. Figure 6d shows that the amplitude of the reaction-rate oscillations was nearly constant when the single step mechanism was used. Only a minor decrease is observed at lean conditions. On the other hand, Lieuwen et al. (1998) reported a small increase in the amplitude when making the mixture leaner. The simulations with the global methane mechanisms and the de-

tailed mechanisms showed that the oscillating fuel consumption-rate amplitudes had a magnitude very similar to the global single-step propane mechanism. The consumption rate of methane was almost equally well predicted by the global mechanisms also for this simulation.

When simulating variations in the inlet flow rate with other amplitudes (cf. section 3.4), the magnitude of the reaction-rate amplitude varied linearly with the amplitude of the variation.

4.6   Variations of inflowing temperature, T_{in}

In the final test series, the responses of the reaction rates to periodic variations in the reactor inlet temperature were simulated. Such temperature oscillations could be due to, for example, acoustic disturbances or other pressure fluctuations (Lieuwen et al., 1998). The results presented here were due to a 5% variation in the inlet temperature, $\dot{m}_{in}/V_R = 500\,\mathrm{kg/(m^3 s)}$ and $T_{mean} = 300\,\mathrm{K}$. The reaction-rate responses of CO_2 and OH obtained from the detailed San-Diego mechanism are shown in Fig. 7. The amplitudes of the reaction-rate oscillations due to an oscillating inlet temperature were for all species small and constant. For CO, CO_2, H_2 and H_2O the reaction-rate amplitudes were almost zero. Only the reaction-rate amplitude of OH differed. When the San-Diego mechanism for propane and the GRI-Mech 3.0 mechanism for methane were applied, the amplitude of the fuel reaction-rate oscillations was one-fourth of the reaction-rate amplitude shown in Fig. 3.

The global propane mechanism showed qualitatively the same behavior as in the work of Lieuwen et al. (1998), that is, a flat profile in the beginning. For the global propane mechanism the variation of the inlet temperature gave a decrease in amplitude of the fuel reaction-rate oscillations as the mean equivalence ratio was decreased. The amplitude were about 30% of the amplitude shown in Fig. 4d. The reaction rate of methane, using the global mechanisms, had oscillations with small and constant amplitude. This amplitude was one-fourth of the reaction-rate amplitude shown in Fig. 3b. Unlike the global propane mechanism, there was no decrease in amplitude of the oscillations as the mean equivalence ratio was decreased.

Simulations with other amplitudes (cf. Sec. 3.4) of the inlet oscillations showed that the magnitude of the reaction-rate amplitudes varied linearly with the amplitude of the variation.

5   DISCUSSION

The perfectly stirred reactor (PSR) is idealized in the sense that the mixing processes are immediate, complete and with no spatial effects. Therefore, the flow and mixing inside the reactor is determined by the residence time and the mass inflow rate, and no further modeling is required. The differences seen between different cases are then due to the inflow parameters and the model of the chemical kinetics. No feedback was included in the PSR model, so the reaction-rate oscillations presented here are only a response of the chemical mechanisms to inlet variations, and the reactor is stable.

Still being models or approximations, we regard the detailed chemical mechanisms as both more general and considerably more accurate than global single-step or few-step mechanisms. It is reasonable to assume that even though detailed chemical mechanisms can be improved, the qualitative results obtained here will not be altered by such improvements. Hence, the behavior seen in simulations with detailed mechanisms is regarded as the qualitatively correct behavior of a PSR, while the differences

seen between detailed and simple mechanisms express deficiencies in the simple mechanisms.

When simulating variations of the inlet equivalence ratio using the detailed chemical mechanisms, the reaction-rate oscillations for OH were damped for $t < 0.1\,\mathrm{s}$, see Fig. 4c. Near the stoichiometric condition a variation of the inflowing equivalence ratio makes the mixture alternatingly rich and lean. For $\phi > 1$ the reaction-rate oscillations will not get larger than the value of the reaction rate at $\phi = 1.0$. As the mixture became leaner, the amplitude of the reaction-rate oscillations grew and became constant. The reaction-rate response of H_2 due to variations of the inlet equivalence ratio was an amplitude that became smaller as the value of ϕ_{mean} was lowered. The main species of the hydrogen reactions is H_2O, for which the reaction-rate oscillations had a constant amplitude.

When imposing oscillations on the reactor inlet temperature, only small oscillations in the reaction rates were predicted. When oscillations were imposed on the inlet mass flow rate, oscillations with larger, nearly constant amplitudes were predicted for all equivalence ratios. Simulations with oscillating inflow equivalence ratio gave reaction-rate oscillations for species other than the fuel that had larger relative differences in the magnitude between stoichiometric and lean conditions. This indicates that equivalence ratio oscillations can cause combustion instabilities under lean conditions. The results from the cases with oscillating inlet flow rate and inflow temperature indicate that combustion instabilities remain unchanged with a non-oscillating decrease in ϕ_{mean}.

The use of the global single-step mechanisms in this study followed up the work by Lieuwen et al. (1998). Such global single-step kinetic mechanisms have a range of validity that is usually quite limited (Westbrook and Dryer, 1981, 1984). Either temperature ranges or equivalence ratios are specified, or both. The performance of a global mechanism in an open reactor depends very much on its parameters: the species concentration exponents, the activation energy and the pre-exponential collision frequency factor. As pointed out by Turns (2000), global mechanisms should be used with much care and only for engineering purposes as approximations. For the global mechanisms used in this study, different tests were performed in order to check model validity. The methane mechanism was tested both with unity and non-unity exponents, while the propane mechanism had exponents of 0.1 and 1.65 with respect to propane and oxygen. The methane mechanism with unity exponents worked for all the tests performed, whereas the propane mechanism gave numerical problems for a wide range of equivalence ratios and reactor residence times, resulting in negative mass fractions and failure of the RADAU5 integrator. When the exponents in the propane mechanism were adjusted towards unity, the resulting reaction-rate oscillations went from nearly zero amplitude at stoichiometric conditions (cf. Fig. 3a) to almost constant amplitude at both stoichiometric and lean conditions (cf. Fig. 3b). The reaction-rate response to imposed oscillations was then similar to that of the detailed mechanism.

In a gas turbine combustion chamber, the inlet pressure and temperature can, for example, be $20\,\mathrm{atm}$ and $800\,\mathrm{K}$, respectively. A simulation of methane combustion with GRI-Mech 3.0, was conducted at these conditions with an oscillating inlet equivalence ratio, and we found that the reaction-rate trends were the same. However, the question remains of how well the chemical mechanism represents the reactions at such high pressures.

6 CONCLUSIONS

A perfectly stirred reactor (PSR) model was used to study reaction-rate responses to varying inlet mass flow rate, temperature and mixture equivalence ratio. Using a PSR, with its idealized mixing

processes and no spatial gradients, makes it possible to isolate effects of chemical kinetics. For all simulations, the mixture was ignited at stoichiometric conditions. Then the mixture was linearly made more and more lean while an oscillation was imposed on one of the inlet variables. Detailed chemical mechanisms were used to model the chemical kinetics. For methane-air combustion, the GRI-Mech 3.0 (Smith et al., 1999) was applied, while for propane-air the San-Diego mechanism (2005) was used. Also global, single-step mechanisms were studied.

When applying the detailed chemical mechanisms, a reduction in mean equivalence ratio led to a reduction in mean fuel consumption rate. Imposed oscillations on either the equivalence ratio, the inflow temperature or the inflow mass flow rate led to oscillations in fuel reaction rate. The amplitude of the fuel reaction rate was virtually unchanged with decreasing mean equivalence ratio.

A gradually leaner mixture with an oscillation of constant percentual amplitude imposed on the inflow gave an increased amplitude of the reaction rate of CO_2 while those of CO and H_2 decreased. The amplitude of the H_2O reaction rate did not change much, whereas that of OH showed an increase.

An linear change in the reaction-rate amplitude with imposed amplitude was observed.

These results were found both for propane and methane, and similar for imposed oscillations on equivalence ratio, inflow temperature and mass flow rate.

Single-step chemical mechanisms gave different results depending on the exponents of the model. With unity exponents for fuel and oxygen, the fuel reaction rate followed the behavior seen with detailed mechanisms when oscillations were imposed.

Most simple chemical mechanisms proposed in the literature have non-unity exponents, such as the one applied by Liuewen et al. (1998). These appear to introduce instable behavior by themselves. Near stoichiometric conditions, the fuel reaction rate was little affected when oscillations were imposed on the inflow. However, when the mean equivalence ratio was lowered below a certain value, the fuel reaction-rate oscillations grew stronger and became larger than seen with the detailed mechanism. This adds to the tendency of giving numerical problems at certain inflow conditions and strict limitations in their domain of use.

ACKNOWLEDGMENTS

REFERENCES

Borghi, R. 1988. Turbulent combustion modelling. *Prog. Energy Combust. Sci*, **14**, 245–292.

Bradley, D., Chin, S. B., Draper, M. S. and Hankinson, G. 1977. *Sixteenth Symposium (International) on Combustion*, 1571–1581.

Chemical Equilibrium Calculator 2007. Avialable at: http://navier.engr.colostate.edu/tools/equil.html. Last visited March 2009.

Cohen, J. M. and Anderson, T. J. 1996. Experimental investigation of near-blowout instabilities in a lean, premixed step combustor. *American Institute of Aeronautics and Astronautics*, paper # 96-0819.

Gran, I. R. and Magnussen, B. F. 1996. A numerical study of a bluff-body stabilized diffusion flames. 2. Influence of combustion modeling and finite-rate chemistry. *Combust. Sci. and Tech.*, **119**, 191–217.

Hairer, E. and Wanner, G. 1996. Solving ordinary differential equations II: Stiff and differential-algebraic problems. *Springer-Verlag, Springer Series in Computational Mathematics*, **2nd rev. ed.**

Hairer, E. and Wanner, G. 2002. RADAU5.
Available at: http://www.unige.ch/ hairer/prog/stiff/radau5.f,
http://pitagora.dm.uniba.it/~testset/solvers/radau5.php. Last visited March 2009.

Kee, R. J., Rupley, F. M., Meeks, E. and Miller, J. A. 1996. CHEMKIN III: A fortran chemical kinetics package for the analysis of gas-phase chemical and plasma kinetics.*Sandia National Laboratories, Livermore Ca*, Report No. UC-405 SAND96-8216.
Available at: http://www.ca.sandia.gov/chemkin/docs.html. Last visited March 2009.

Lieuwen, T. C., Neumeier, Y. and Zinn, B. T. 1998. The role of unmixedness and chemical kinetics in driving combustion instabilities in lean premixed combustors. *Combust. Sci. and Tech.*, **135**, 193–211.

Myhrvold, T. and Gruber, A. 2006. Modelling of combustion instabilities with SPIDER. Research progress evaluation, unsteady reactor model, and further work. Technical report TR A6300, SINTEF Energy Research, Trondheim, Norway.

Poinsot, T. and Veynante, D. 2005. Theoretical and numerical combustion. *R. T. Edwards*, **2nd ed.**

San-Diego mechanism 2005. Available at: http://maeweb.ucsd.edu/~combustion/cermech/. Last visited March 2009.

Shih, W. P., Lee, J. G. and Santavicca, D. A. 1996. Stability and emissions characteristics of a lean premixed gas turbine combustor. *Twenty-Sixth Symposium (International) on Combustion*, 2771–2778.

Smith, G. P., Golden, D. M., Frenklach, M., Moriarty, N. W., Eiteneer, B., Goldenberg, M., Bowman, C. T., Hanson, R. K., Song, S., Gardiner, W. C., Lissianski, Jr., V. V. and Qin, Z. 1999. GRI-Mech 3.0. Available at: http://www.me.berkeley.edu/gri_mech/. Last visited March 2009.

Turns, S. R. 2000. An introduction to combustion, concepts and applications. *McGraw-Hill*, **2nd ed.**

Westbrook, C. K. and Dryer, F. L. 1981. Simplified reaction mechanisms for the oxidation of hydrocarbon fuels in flames. *Combust. Sci. and Tech.*, **27**, 31–43.

Westbrook, C. K. and Dryer, F. L. 1984. Chemical kinetic modeling of hydrocarbon combustion. *Prog. Energy Combust. Sci.*, **10**, 1–57.

Williams, F. A. 1985. Combustion theory: The fundamental theory of chemically reacting flow systems. *The Benjamin/Cummings Publishing Company*, **2nd ed.**

Zinn, B. T. and Lieuwen, T. C. 2005. Combustion instabilities: Basic concepts. In: Lieuwen, T. C. and Yang, V. (eds). Combustion instabilities in gas turbine engines: Operational experience, fundamental

mechanisms, and modeling. *Prog. in Astronautics and Aeronautics*, **210**: 3–26.

Table 1: Various combinations of constants and variables in the τ-expression (see Eq. (4)).

Mode	Constants	Variables	Extra information needed
I	$V_R, \dot{m}_{in}$	$m_R = \rho V_R \sim \rho, \tau \sim m_R \sim \rho$	No
II	V_R, τ	$m_R = \rho V_R \sim \rho, \dot{m}_{in} = m_R/\tau \sim \rho$	No
III	$\tau, \dot{m}_{in}, m_R = \tau \dot{m}_{in}$	$V_R = m_R/\rho \sim 1/\rho$	No
IV	$\dot{m}_{in}$	V_R, m_R, τ	dV_R/dt
V	τ	$V_R, m_R, \dot{m}_{in}$	dV_R/dt
VI	m_R	$V_R, \tau, \dot{m}_{in}$	dV_R/dt
VII	V_R	$m_R, \tau, \dot{m}_{in}$	dV_R/dt

Table 2: Values for the constants in Eq. (5) (Bradley, 1977, Westbrook, 1981, 1984).

Fuel	A $[(kg/m^3)^{1-m-n}/s]$	m	n	T_a [K]
Methane(1)	$1.4704 \cdot 10^{12}$	1	1	17404
Methane(2)	$3.0 \cdot 10^{13}$	0.7	0.8	23666
Propane	$4.773 \cdot 10^8$	0.1	1.65	15098

Table 3: Values of a in Eq. (6).

Mixture	Mechanism	Constant a
Propane-air	Single-step	$4.5 \cdot 10^6$
Propane-air	San-Diego	$6.8 \cdot 10^6$
Methane-air	Single-step(1)	$3.2 \cdot 10^6$
Methane-air	Single-step(2)	$3.9 \cdot 10^6$
Methane-air	GRI-Mech 3.0	$8.2 \cdot 10^6$

List of Figures

16

Figure 1: Perfectly stirred reactor.
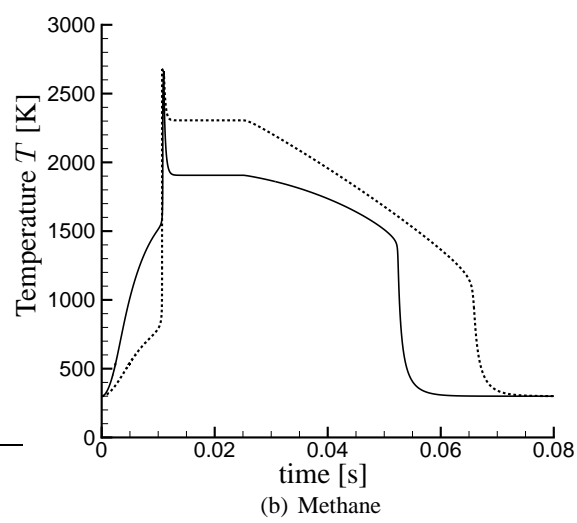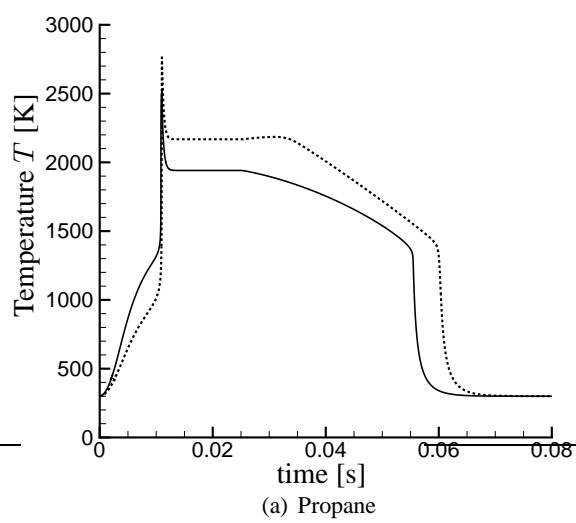
(a) Propane

(b) Methane

Figure 2: Ignition and extinction of propane and methane. Dotted line: single-step global mechanism. Solid line: detailed mechanism.
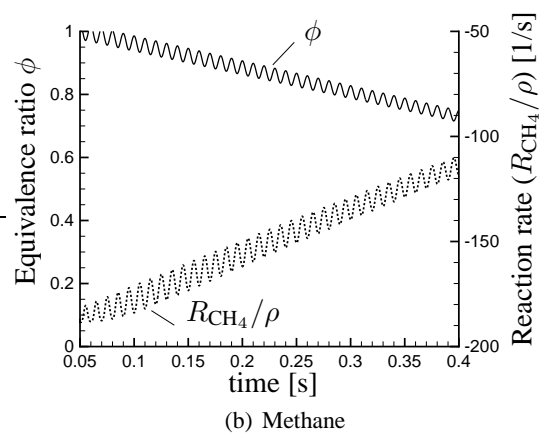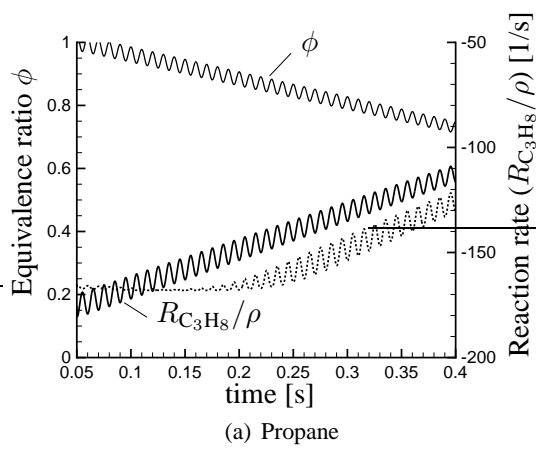
Figure 3: Reaction-rate response to a 2.5% variation about ϕ_{mean}. Dotted line: single-step global mechanism. Solid line: detailed mechanism.
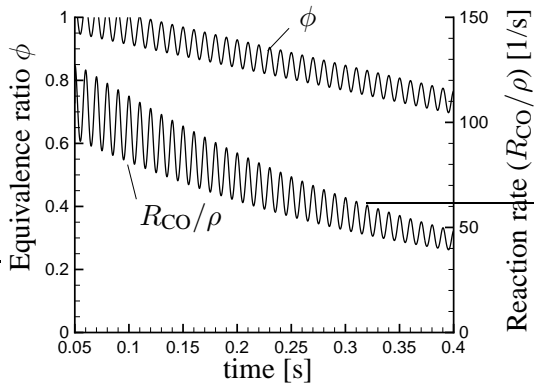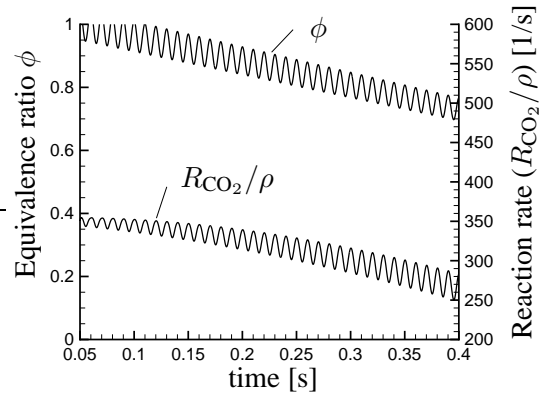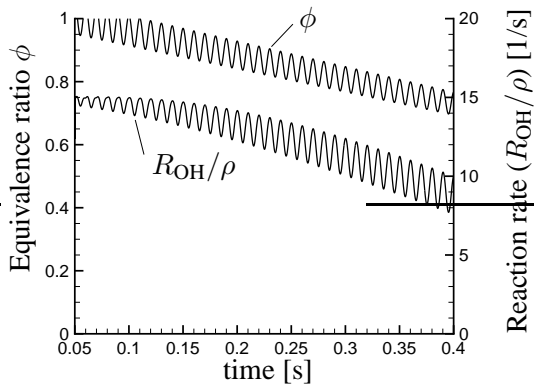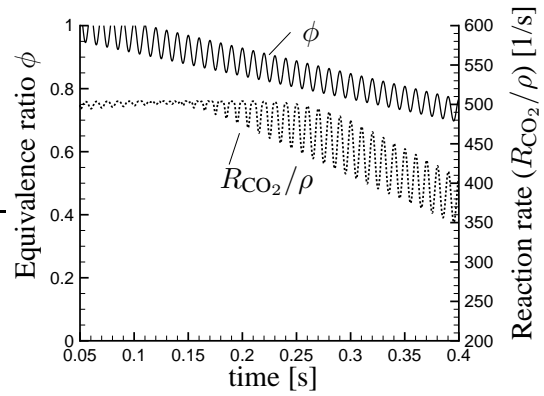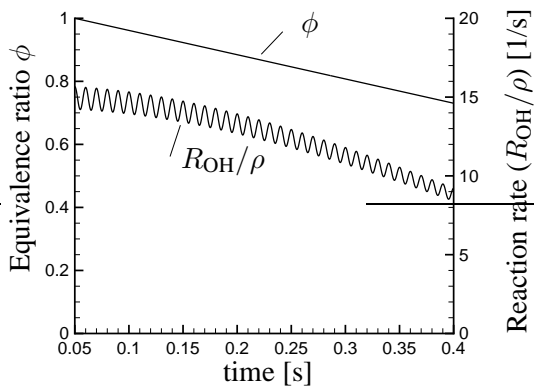
Figure 4: Reaction-rate response to a 5% variation about ϕ_{mean}.
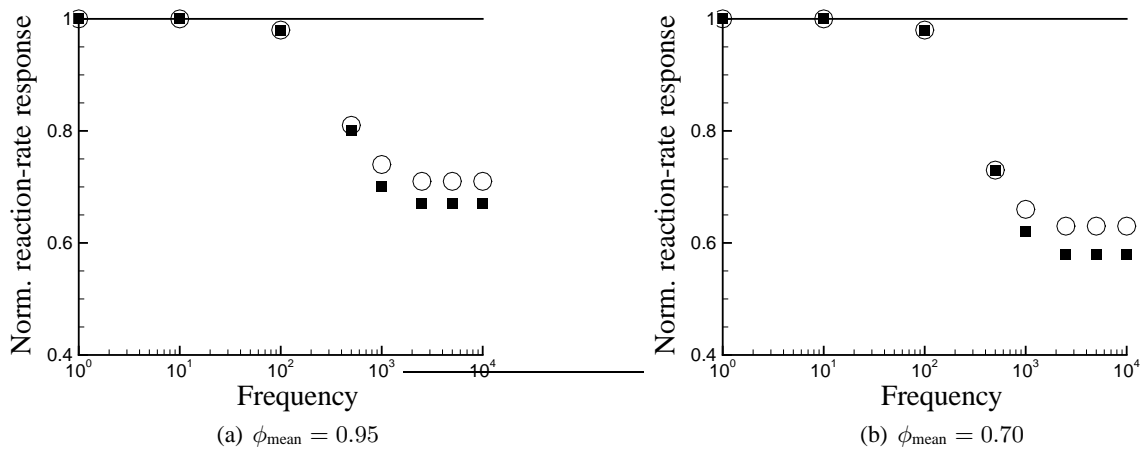
Figure 5: Frequency dependence of the normalized reaction-rate responses (i.e., the response at $f = 0\,\mathrm{Hz}$) for C_3H_8 and H_2O to equivalence ratio oscillations using the San-Diego mechanism (2005). $P = 1\,\mathrm{atm}$, $T_{\mathrm{in}} = 300\,\mathrm{K}$ and $\dot{m}_{\mathrm{in}}/V_R = 400\,\mathrm{kg/(m^3s)}$. Circle: C_3H_8. Square: H_2O.
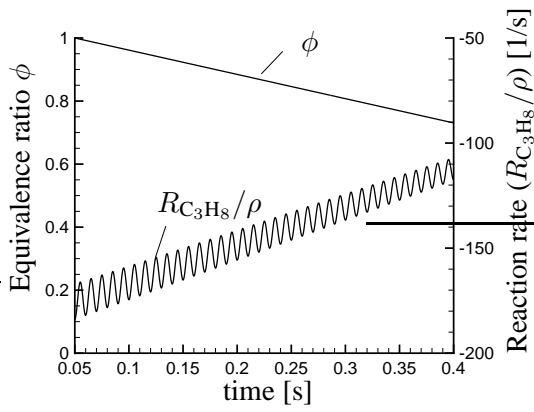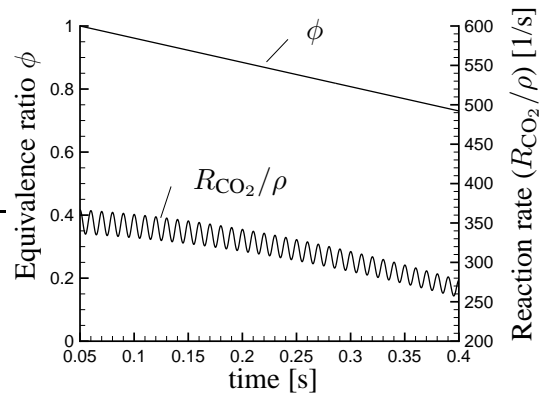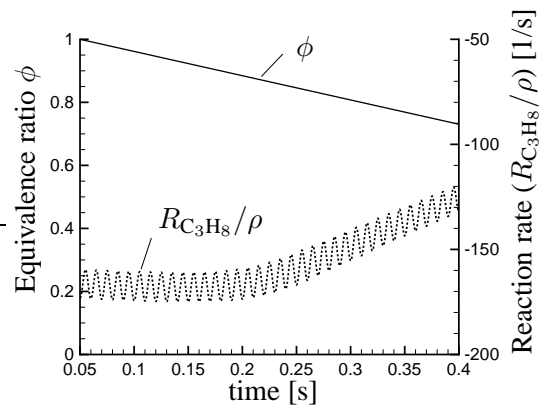
Figure 6: Reaction-rate response to a 5% variation about $(\dot{m}_{\text{in}}/V_{\text{R}})_{\text{mean}}$.
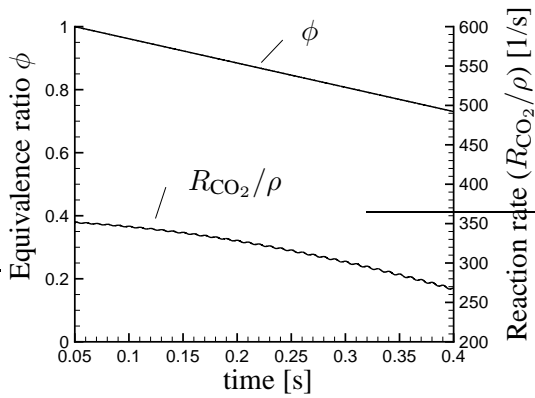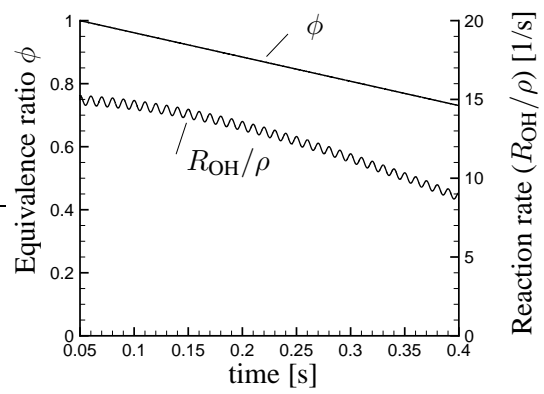
Figure 7: Reaction-rate response to a 5% variation about T_{mean}.